Lateral Quantization of Two-Dimensional Electron States by Embedded Ag Nanocrystals

K. Schouteden* and C. Van Haesendonck

Laboratory of Solid-State Physics and Magnetism, K. U. Leuven, BE-3001 Leuven, Belgium

(Received 25 May 2011; published 17 February 2012)

We show that quantization of image-potential state (IS) electrons *above* the surface of nanostructures can be experimentally achieved by Ag nanocrystals that appear as stacking-fault tetrahedrons (SFTs) at Ag(111) surfaces. By means of cryogenic scanning tunneling spectroscopy, the $n = 1$ IS of the Ag(111) surface is revealed to split up in discrete energy levels, which is accompanied by the formation of pronounced standing wave patterns that directly reflect the eigenstates of the SFT surface. The IS confinement behavior is compared to that of the surface state electrons *in* the SFT surface and can be directly linked to the particle-in-a-box model. ISs provide a novel playground for investigating quantum size effects and defect-induced scattering *above* nanostructured surfaces.

DOI: 10.1103/PhysRevLett.108.076806 PACS numbers: 73.22.−f, 68.37.Ef, 73.20.−r

Image-potential states (ISs) are known as the intriguing series of subsequent electron layers that exist *above* surfaces, i.e., in the narrow region in between the crystal surface potential and the Coulomb image potential at the vacuum side. These states have been the subject of extensive theoretical [1–3] and experimental investigations including, in particular, photoemission spectroscopy [4–7]. Their two-dimensional (2D) free-electron-like nature offers promising yet unexploited possibilities: In case IS electrons can be effectively confined by a 2D scattering potential, they provide a potential novel playground for fundamental investigations of quantum mechanical finite size effects *above* nanostructured surfaces. Dedicated studies require the use of local probe techniques rather than of spatially averaging techniques [5].

Scanning tunneling microscopy (STM) combined with scanning tunneling spectroscopy (STS) allows us to reliably probe both the structural and electronic properties of surfaces with high spatial and energy resolution. Surprisingly, only a few STM/STS investigations of the scattering behavior of IS electrons have been reported so far. Wahl *et al.* have shown that step edges at Cu(100) surfaces yield an effective scattering potential for IS electrons, allowing us to determine the parabolic energy dispersion of the ISs by mapping the resulting standing wave (SW) patterns [8]. However, reports on quantization of IS electrons, e.g., above the surface of nanoparticles, are still lacking. Only very recently, we observed that IS electrons form SW patterns above nanosized Co islands on Au(111) surfaces due to scattering by the island edges, which is accompanied by a small but significant shift of the IS energies to higher energies [9]. More spectacular outcomes are waiting to be discovered, yet this novel area of research remains unexplored so far.

This is in striking contrast to the amount of studies of the well-known Shockley surface states (SSs), a 2D electron gas that is restricted to the top atomic layers of its host surface. In the last two decades, SSs received enormous and yet undiminished scientific interest, since it was shown that they can be easily confined by, e.g., monatomic steps, adatoms, and other adsorbates [10–12]. Although, from a theoretical point of view, IS quantization by IS electrons can be expected due to the obvious similarities with SS electrons, its experimental realization appears to be far from trivial, as it requires additional conditions to be fulfilled when compared to SS electrons. First, it was predicted by A. G. Borisov *et al.* that confinement of IS electrons near the surface of nanostructures requires the work function of the confining nanostructure to be lower than that of its environment [13]. Second, because of the narrow energy window provided by the IS ''energy bands'' (compared to the large energy window in which SS electrons exist), only a proper combination of the nanostructure size and electron effective mass can yield a detectable number of quantized eigenstates. Third, the confining nanostructure needs to have a quasiperfect shape to ensure that the confined IS electrons quantize in resolvable discrete energy levels in the narrow IS energy window. Any deviation from a perfect crystallographic (i.e., polygonal) shape will hamper the formation of pronounced quantized states.

In this Letter, we show that all three required conditions are fulfilled for Ag nanocrystals that form spontaneously as stacking-fault tetrahedrons (SFTs) in Ag(111) films, which hence form a unique object for investigation. SFTs are three-dimensional nanocrystalline defects of which one triangular surface is exposed at the Ag(111) surface [see Fig. 1(b)], while—below the surface—the SFT is ''decoupled'' from the surrounding Ag(111) substrate by three triangular {111}-stacking-fault planes. Our STM/STS study reveals for the first time the remarkable quantization of IS electrons due to the lateral confinement experienced near the exposed surface of nanoparticles, i.e., nanometer-sized SFTs. Because of the perfect triangular shape of the exposed SFT surface, quantization is accompanied by the formation of pronounced energy-dependent SW patterns

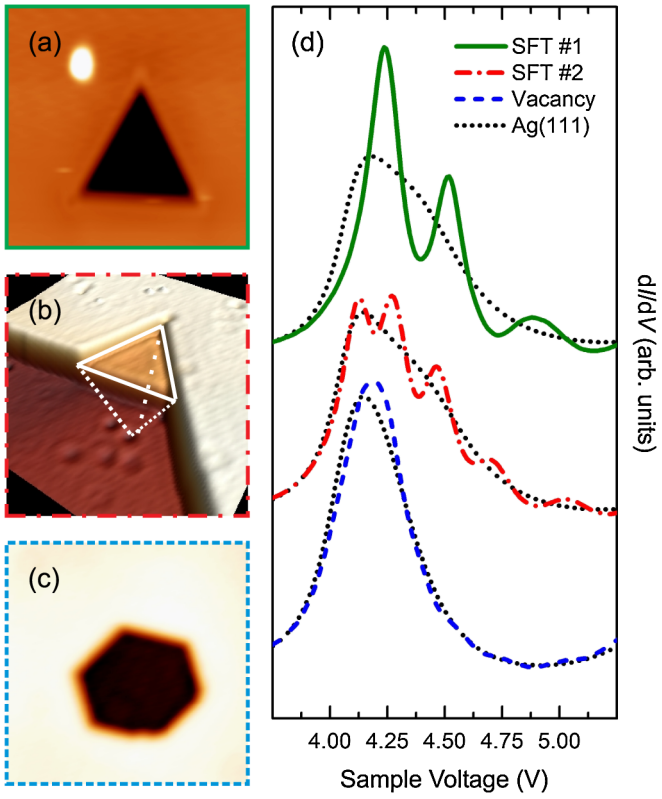

FIG. 1 (color online). (a) 14×14 nm^2 topography image of a nanosized SFT (side length is around 7 nm). (b) 40×40 nm^2 3D view of a larger SFT (side length is around 11 nm). White solid and dotted lines illustrate the 3D shape of the SFT at and below the surface. (c) 12×12 nm^2 image of a monatomic vacancy island created by mild Ar^+ bombardment. (d) dI/dV spectra of the $n = 1$ IS recorded above the nanostructures presented in (a) and (b) ($V = 3.0$ V, $I = 10.0$ nA) and (c) ($V = 3.0$ V, $I = 2.0$ nA). A spectrum recorded at the surrounding Ag(111) surface is given as a reference for each nanostructure. The curves are offset for clarity.

that are resolved in detail in maps of the local density of states (LDOS). Finally, we compare the confinement behavior of the IS and of the SS electrons at the SFT surface and are able to directly link this behavior to the 2D particle-in-a-box model.

Atomically flat Ag(111) films on mica [14] are cleaned by repeated Ar^+ sputtering and annealing cycles. Nanometer-sized Ag vacancy islands are created by means of additional (few seconds) Ar^+ sputtering. STM and STS measurements are performed with an ultrahigh vacuum (base pressure in the 10^{-11} mbar range) STM setup (Omicron Nanotechnology) at 4.5 K using W tips [9]. Spectra of dI/dV versus V (V is the voltage applied to the sample, while the STM tip is virtually grounded) are acquired with an open (for SS measurements) or closed (for IS measurements) feedback loop via lock-in detection at a modulation frequency of 840 Hz and with a modulation amplitude in the 20 to 50 mV range. Curves are recorded with a grid size of 200×200 points, from which color maps that directly reflect the LDOS can be produced at selected values of V. Image processing is performed by Nanotec WSXM [15].

The Ag(111) surface accommodates various types of dislocations, including screw, edge, and Lomer-Cottrell dislocations [16,17]. When compared to other fcc metals, Ag has an exceptionally small stacking-fault energy [18] so that dislocations are observed more frequently in Ag films. Figures 1(a) and 1(b) present a more exotic type of dislocation with the shape of an equilateral triangle (side length is around 7 and 11 nm, respectively), about 0.1 nm lower than the surrounding upper Ag(111) terrace. This triangular surface is one of the four surfaces of a nanometer-sized SFT [16,17]. Figure 1(c) presents a hexagonal monatomic vacancy island.

In Fig. 1(d), we present dI/dV spectra recorded at the center of the nanostructures shown in Figs. 1(a)–1(c). A spectrum of the surrounding Ag(111) surface is added as a reference for all measurements (the precise energy at which ISs are recorded depends on the geometry of the tip apex and hence varies from tip to tip). Remarkably, whereas the $n = 1$ IS (n is the principal quantum number [1]) of the vacancy island is similar to that of the surrounding Ag(111) surface, we find that the $n = 1$ IS of both SFTs is split up into multiple discrete states. Moreover, while the larger SFT in Fig. 1(b) reveals 5 discrete states, the smaller SFT in Fig. 1(a) exhibits only 3 discrete states with larger energy separations. Quantization of the $n = 1$ IS is observed for all investigated SFTs and becomes less pronounced with increasing SFT size. This size dependence is consistent with that of a 2D electron gas that is confined to a 2D scattering potential [10–12]. Our STS measurements hence provide direct experimental evidence for the lateral confinement of IS electrons by the surface of embedded Ag nanocrystals. It must be noted that higher-order ISs do not reveal any quantization caused by the presence of the SFT (data not shown).

The origin of the observed confinement can be related to the difference in work function of the Ag nanocrystal when compared to the surrounding Ag(111) surface [9,13]. Indeed, our STS spectra reveal that higher-order ISs of the SFT occur at about 50 meV lower energies (data not shown). Following the work of Lin *et al.*, this implies that the SFTs have a lower work function when compared to the surrounding Ag(111) surface [19]. This reduced work function can be related to a different stacking of the Ag atoms in the nanocrystalline SFT, i.e., an increased distance between the successive atomic layers in the SFT [20].

In addition, we note that voltage-dependent SW patterns formed by scattered $n = 1$ IS electrons are observed near 1D dislocations (data not shown) at the lower terrace side only, providing direct proof that $n = 1$ IS electrons are effectively scattered by dislocations. On the other hand, we find that $n = 1$ IS electrons do not form SWs at monatomic steps, in contrast to earlier observations for

Cu(100) surfaces [8]. This difference can be related to the fact that the $n = 1$ IS of Cu(100) lies well within the surface band gap, while that of Ag(111) lies close to the upper surface band gap edge [4]. The applied electric field (determined by the sample voltage and current set point) induces a Stark shift of the IS to higher energies [3], i.e., above the upper surface band gap edge. The IS hence becomes a (field emission) resonance state that experiences coupling with underlying Ag(111) bulk states. This implies that the $n = 1$ IS electrons scatter to Ag bulk states rather than backwards, which explains the absence of SWs at monatomic Ag(111) steps. Similarly, whereas monatomic steps act as a scattering potential for SS electrons [11], SW formation due to scattering of $n = 1$ IS electrons at the boundaries of monatomic vacancy islands such as the one in Fig. 1(c) is not observed. The above indicated absence of resolvable scattering and quantization for higher-order ISs ($n > 1$) at SFTs and 1D dislocations can be related to an enhanced coupling to underlying bulk states of the Ag(111) surface at higher energies [3].

Next, we investigated the confinement behavior of the $n = 1$ IS above a SFT into more detail by recording LDOS maps of the SW patterns formed by the scattered IS electrons, which are compared to that of SWs formed by SSs at the same SFT surface, i.e., the one shown in Fig. 1(a). Figure 2 presents an overview of a series of such LDOS maps of SSs [Figs. 2(a)–2(f)] at the SFT and ISs [Figs. 2(i)–2(n)] above the SFT, together with the dI/dV spectra of Figs. 2(g) and 2(h) recorded at the locations indicated in Figs. 2(e) and 2(k), respectively. The Ag(111) spectra in Figs. 2(g) and 2(h) reveal the SS onset energy E_0 at -67 meV [11] and the $n = 1$ IS maximum at energy E_1 around 4.2 eV, respectively.

Lateral confinement of the SS electrons to the SFT surface causes the SS energy band to split up into a series of discrete energy levels [21] following the 2D particle-in-a-box model:

$$E_{N,M} = E_0 + \frac{\lambda_{N,M}}{m^*\Omega}, \qquad N, M = 1, 2, 3, \ldots, \tag{1}$$

where Ω is the effective area of the confining surface, $m^* \approx 0.42 m_e$ [11] is the effective electron mass, and the $\lambda_{N,M}$ denote the eigenvalues that depend solely on the shape of the box, i.e., an equilateral triangle [22]. For a finite height of the confining potential, Ω can become somewhat larger than the actual surface area of the nanoparticle because of the "spillout" of the particle's wave functions [11]. When fitting the maxima in Fig. 2(g) to Eq. (1) and our experimental LDOS maps to theoretical LDOS maps relying on the particle-in-a-box software (available via Ref. [23]) developed by K.-F. Braun [24] (the Schrödinger equation is solved by treating scattering centers as zero-range potentials), perfect agreement is achieved for $\Omega = 27$ nm^2, corresponding to a side length L of 7.9 nm. This is consistent with the STM topography in Fig. 1(a) when taking into account a limited spillout for the LDOS maps (see the Supplemental Material for simulated LDOS maps [25]). The fitting reveals that

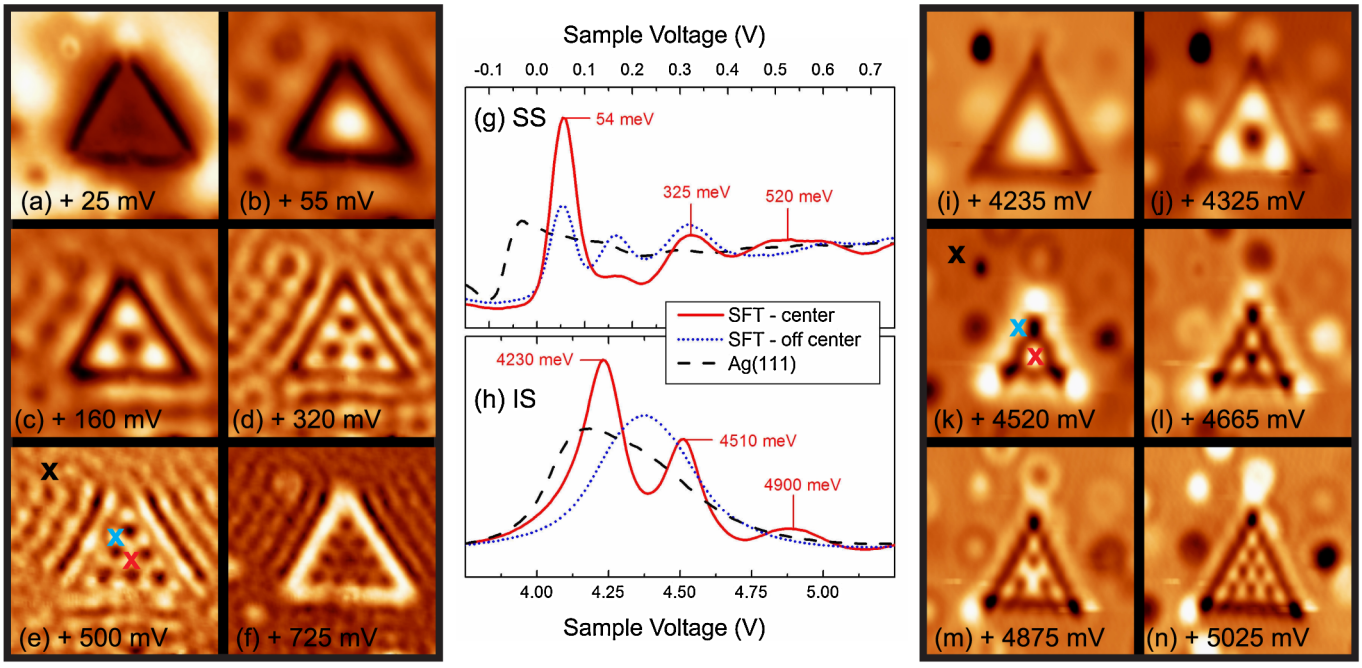

FIG. 2 (color online). (a)–(f) 13×13 nm^2 LDOS maps of SSs in a SFT; a movie is available online ($V = +0.75$ to -0.15 V) [25]. (g) dI/dV spectra recorded at the indicated locations in (e) ($V = 1.0$ V, $I = 1.0$ nA). (h) dI/dV spectra recorded at the indicated locations in (k) ($V = 3.0$ V, $I = 10.0$ nA). (i)–(n) 13×13 nm^2 LDOS maps of ISs above a SFT; a movie is available online ($V = +4.0$ to $+5.2$ V) [25].

Figs. 2(b) and 2(c) reflect the $(N = 1, M = 2)$ and $(N = 1, M = 3)$ eigenstates [26], respectively, while LDOS maps at higher energies typically reflect a superposition of multiple eigenstates.

In contrast to SS SWs, SWs due to scattered IS electrons can only be observed *above* the SFT [see Figs. 2(i)–2(n)]. The mean energy separation between the successive quantized states probed at the SFT center [see Figs. 2(g) and 2(h)] appears to be comparable for the SSs (230 ± 40 meV) and the $n = 1$ ISs (340 ± 60 meV). Following Eq. (1), with E_0 now replaced by E_1, the product $m^*\Omega$ should then be comparable, as well, for the SS and the $n = 1$ IS electrons. Taking into account the different effective electron mass reported for both types of electron states ($m^* \approx 0.42 m_e$ [11] for SS electrons, while $m^*/m_e = 1.3$ [6] for IS electrons), this would imply that IS electrons experience a considerably different effective area Ω than SS electrons.

According to the ''ideal'' particle-in-a-box model, similar SW patterns are expected to occur for a comparable $m^*\Omega$ product at comparable energy separations for both SS and IS electrons. Indeed, at energies close to E_0 and E_1, the observed IS SW patterns exhibit a clear resemblance to the SW patterns of the SSs [compare Figs. 2(b) and 2(c) to Figs. 2(i) and 2(j), respectively]. At higher energies, the IS SW patterns appear to be different from the patterns of the SSs {see, e.g., Fig. 2(k), which reflects the $(N = 1, M = 5)$ eigenstate [26]}. Upon more careful inspection of Figs. 2(k)–2(n), it can be seen that part of the SW pattern becomes somewhat hidden in the SFT boundaries. This can be related to the increasing influence of tip convolution effects with increasing energy (and hence tip-sample distance). Keeping this in mind, we find that the energy maxima in Fig. 2(h) and the experimental LDOS maps are consistent with Eq. (1) and the theoretical LDOS maps [23,24], respectively (see the Supplemental Material for simulated LDOS maps [25]), using $m^*\Omega = 21\ \mathrm{nm}^2 m_e$ and $E_1 = 4.19$ eV. Taking $m^*/m_e = 1.3$, as obtained for the $n = 1$ IS of Ag(111) by photoemission measurements [6], yields $L = 6.1$ nm. This is smaller than the side length obtained above for the SS confinement. On the other hand, the lateral size of the SW patterns formed by SS and IS electrons in Figs. 2(a)–2(f) and Figs. 2(i)–2(n) appears to be the same within the experimental error. It is therefore more reasonable to assume a modified effective electron mass for the IS electrons (which can be attributed to the above indicated different stacking of the Ag atoms in the nanocrystalline SFT) rather than a reduced effective surface area. Taking $L = 7.9$ nm yields $m^*/m_e = 0.78$ for the $n = 1$ IS. This is still larger than the m^*/m_e values reported for SS electrons. Detailed calculations similar to those of A. G. Borisov *et al.* [13], with the additional complication of a less symmetric confinement potential, will be needed to achieve a full quantitative description of our experimental results. Hereby, electron scattering at the stacking-fault planes of the SFT below the surface [27] needs to be considered. Finally, the sensitivity of the quantized ISs to the applied electric field may influence our results, as well. We observed a gradual Stark shift of about 60 meV upon increasing the current from 0.1 to 10.0 nA (the sample voltage set point is the same), which is accompanied by a small deformation of the IS patterns across the SFT surface (see the Supplemental Material [25]).

In conclusion, our STM/STS measurements reveal that $n = 1$ IS electrons can be confined to the surface boundaries of defect-related nanoparticles. Lateral confinement causes the IS energy band to split into a series of discrete energy levels, which is accompanied by the formation of energy-dependent SWs that reflect the wave functions of the confining area. Our findings open new perspectives for the yet unexploited research on scattering and confinement of 2D electron gases provided by IS electrons above specific, individual scattering centers. In particular, one possibility is to rely on the spin polarization of the IS electron gas above a ferromagnetic material [28] to investigate spin-dependent scattering at the boundaries of magnetic nanostructures. Another possibility is to create a spatially modulated confinement of the electron gas by adsorbing a nanoporous molecular network which induces a spatial modulation of the work function.

This work has been supported by the Research Foundation—Flanders (FWO, Belgium), as well as by the Belgian Interuniversity Attraction Poles (IAP) and the Flemish Concerted Action (GOA) research programs. K. S. is a postdoctoral researcher of the FWO.

*Koen.Schouteden@fys.kuleuven.be

[1] P. M. Echenique and J. B. Pendry, J. Phys. C **11**, 2065 (1978).
[2] E. V. Chulkov, V. M. Silkin, and P. M. Echenique, Surf. Sci. **437**, 330 (1999).
[3] S. Crampin, Phys. Rev. Lett. **95**, 046801 (2005).
[4] S. Schuppler *et al.*, Phys. Rev. B **46**, 13 539 (1992).
[5] R. Fischer, Th. Fauster, and W. Steinmann, Phys. Rev. B **48**, 15 496 (1993).
[6] K. Giesen *et al.*, Phys. Rev. B **35**, 975 (1987).
[7] W. Berthold *et al.*, Phys. Rev. Lett. **88**, 056805 (2002).
[8] P. Wahl *et al.*, Phys. Rev. Lett. **91**, 106802 (2003).
[9] K. Schouteden and C. Van Haesendonck, Phys. Rev. Lett. **103**, 266805 (2009).
[10] M. F. Crommie, C. P. Lutz, and D. M. Eigler, Science **262**, 218 (1993).
[11] J. Li *et al.*, Phys. Rev. Lett. **80**, 3332 (1998).
[12] H. Jensen *et al.*, Phys. Rev. B **71**, 155417 (2005).
[13] A. G. Borisov *et al.*, Phys. Rev. B **76**, 121402 (2007).
[14] N. Vandamme *et al.*, J. Phys. Condens. Matter **15**, S2983 (2003).
[15] I. Horcas *et al.*, Rev. Sci. Instrum. **78**, 013705 (2007).
[16] J. F. Wolf and H. Ibach, Appl. Phys. A **52**, 218 (1991).

[17] D. Hull and D. J. Bacon, *Introduction to Dislocations* (Butterworth-Heinemann, Oxford, 2001).
[18] B.-J. Lee, J.-H. Shim, and M. I. Baskes, Phys. Rev. B **68**, 144112 (2003).
[19] C. L. Lin *et al.*, Phys. Rev. Lett. **99**, 216103 (2007).
[20] W. Li and D. Y. Li, Mater. Sci. Technol. **18**, 1057 (2002).
[21] T. Uchihashi, K. Kobayashi, and T. Nakayama, Phys. Rev. B **82**, 113413 (2010).
[22] H. R. Krishnamurthy, H. S. Mani, and H. C. Verma, J. Phys. A **15**, 2131 (1982).
[23] K.-F. Braun, Calculation of Standing Wave Pattern and Image Processing, http://www.kai-felix-braun.de/program.htm (2006).
[24] K.-F. Braun and K.-H. Rieder, Phys. Rev. Lett. **88**, 096801 (2002).
[25] See Supplemental Material at http://link.aps.org/supplemental/10.1103/PhysRevLett.108.076806 for simulated LDOS maps and visualizations of the IS patterns at different settings of the current.
[26] N. A. Stavropoulos and D. K. Morr, Phys. Rev. B **71**, 140501 (2005).
[27] O. Kurnosikov, H. J. M. Swagten, and B. Koopmans, Phys. Rev. Lett. **106**, 196803 (2011).
[28] A. Kubetzka, M. Bode, and R. Wiesendanger, Appl. Phys. Lett. **91**, 012508 (2007).